Time-varying motor control strategy for proximal-to-distal sequential energy distribution: Insights from baseball pitching

Kozo Naito

Corresponding author: Kozo Naito

Faculty of Education, Soka University

Postal address: 1-236 Tangi-machi, Hachioji 192-8577, Japan

Phone number: +81-042-691-9378

Fax number: +81-042-691-9332

Email address: knaitoh@soka.ac.jp

Key words: Baseball, pitching, induced-power analysis, mechanical energy, coordination, multi-joint system

Abstract:

The importance of a proximal-to-distal (P-D) sequential motion in baseball pitching is generally accepted; however, the mechanisms behind this sequential motion and motor control theories that explain which factor transfers mechanical energy between the trunk and arm segments are not completely understood. This study aimed to identify the energy distribution mechanisms among the segments and determine the effect of the P-D sequence on the mechanical efficiency

of the throwing movement, focusing on the time-varying motor control. The throwing motions of 16 male collegiate baseball pitchers were measured by a motion capture system. An induced power analysis was used to decompose the system mechanical energy into its muscular and interactive torque-dependent components. The results showed that the P-D sequential energy flow during the movement was mainly attributed to three different joint controls of the energy-generation and muscular torque- and centrifugal force-induced energy-transfer. The trunk muscular torques provided the primary energy sources of the system mechanical energy, and the shoulder and elbow joints played the roles of the energy-transfer effect. The mechanical energy expenditure on the throwing hand and ball accounted for 72.7% of the total muscle work generated by the trunk and arm joints (329.2 J). In conclusion, the P-D sequence of the throwing motion is an effective way to utilize the proximal joints as the energy source and reduce muscular work production of the distal joints. This movement control assists in efficient throwing, and is consistent with the theory of the leading joint hypothesis.

1. Introduction

A proximal-to-distal (P-D) sequential motion is a phenomenon that can be observed in a large variety of upper and lower limb motions in human. This motion pattern, where the motion is initiated by the proximal segments and the more distal segments starts its motion when the adjacent proximal segment reaches its peak velocity (Putnam, 1993), is observed in a broad

range of motions, such as throwing, striking, and kicking. A general notion of the P-D sequence is presented in a multi-disciplinary overview that includes research from various domains (Serrien and Baeyens, 2017). The importance of the P-D sequence in human upper and lower limb motions is generally accepted (Putnam, 1993; Van den Tillaar and Ettema, 2009; Wagner et al., 2012); however, the interpretations of the P-D sequential motion of throwing and striking actions are not entirely consistent. For example, the summation of the speed principle (Bunn, 1972), which states that the system will achieve an optimum endpoint velocity if motion of the distal segment begins at the time of maximum speed of the proximal segment, is frequently applied to a general explanation of an ideal motion pattern of throwing and striking. However, by itself, it does not uniquely specify this sequential pattern, because when the joint velocities of the shoulder, elbow, wrist, and fingers reach a peak speed at the same time at a fully extended orientation, the fingertip speed will be greater than that when the peak joint velocities of each joint occur at different times (Hatsopoulos et al, 2010). A kinetic account of P-D sequencing of throwing and striking suggests that the interaction torques acting on a joint originating from the velocity and acceleration of neighboring joints can explain this sequential pattern. This motion pattern could result in transfer of energy or momentum from the proximal to distal segments, thus achieving greater velocity of the terminal segment (Kreighbaum and Barthels, 1996; Putnam, 1993). However, how the interaction torque makes throwing more efficient is not sufficiently evident, because the interaction torque analysis is not a direct approach for the

calculation of the transfer of kinetic energy. Hi-speed overarm throwing is the fastest motion in human and a distinctive human behavior (Roach et al., 2013). Joint control in this motion is complex because of the requirement of multi-joint coordination with rapid upper-limb rotation, with the aim of applying great velocity or power to the throwing hand. Understanding of the joint coordination during fastball throwing is helpful in gaining the advanced knowledge on the organizing principle of multi-joint motor control through the P-D sequence.

One interesting hypothesis is that the movement organization of the multi-joint limb system might be based on the leading joint hypothesis (LJH) theory (Dounskaia, 2005; Dounskaia, 2011). This theory states that multi-joint coordination is achieved by hierarchical control, in which the motion at the leading joint is caused by the muscle activity acting at the proximal joint, and this joint produces an interaction torque that drives the subordinate joints. These subordinate joints then exploit or modify this interaction torque to achieve the desired task. A previous interaction torque analysis suggests that the kinetic behavior of the throwing limb is consistent with the LJH, in which the proximal joint torque (e.g., trunk) creates a dynamic foundation for the entire limb motion, and the interaction torque at the subordinate joints (e.g., elbow) generated by the proximal joint is utilized to fulfill the task demand (Hirashima et al., 2007). Interaction torque analyses are useful for explaining of how a motion pattern is created by the mechanical factors (e.g. muscular or interactive torques). However, these

analyses cannot generally determine the mechanical factor that contributes to the energy transfer, or explain what a kind of criteria (e.g. mechanical efficiency) is used to organize the motion. Bernstein's theory (1967) states that the control strategy used by the central nervous system (CNS) in multi-joint limb movements exploits the mechanical forces owing to segment interactions, enhancing the efficiency of muscular forces. A motor skill study suggested that learning and control are associated with a propensity to reduce the energy cost of achieving the task-goal with practice and to adapt movements to task constraints using an energy-efficient preferred mode (Sparrow et al., 1999). Based on their suggestions, we assume that an investigation from the perspective of mechanical energy flow would provide key insights for elucidating the joint control strategy. Especially, we focus on the mechanical efficiency of movement as the key factor for understanding appropriate joint coordination. An energetic approach can help justify the effectiveness of the LJH more clearly than kinematic and kinetic approaches, because it evaluates the direct relation between the accelerating/decelerating joint control and movement efficiency.

An induced power analysis (IPA), which is a method that decomposes mechanical energy into causal joint work and transferred energy owing to intersegmental joint force, has been recently used to investigate multi-articular coordination in throwing and striking motions (Aguinaldo and Escamilla, 2020, Naito et al., 2011). The IPA can be used to determine the cause–effect

relationship between the energy gain, sources, and distribution mechanisms through muscular and interaction torques, thus determining the mechanical efficiency of movement. This approach can detect coordination between the joints to achieve task-specific goals. For example, Fregly and Zajac (1996) determined the detailed mechanism of muscle joint torque function to propel the crank in seated ergometer pedaling, focusing on the differences in the roles of the proximal and distal joints. The mechanisms of the joint torque that exert work to the system and how the joints synergistically function to deliver energy to a target object may provide new information on a control strategy for the P-D sequential motion. In a multi-joint-link system, the motion of a segment resulting from a joint torque generally induces the motion of the adjacent segment as well as that of a non-adjacent segment through intersegmental forces (Zajac et al., 2002). To clarify the complicated mechanical interaction between adjacent and non-adjacent segments, an analysis should fully decompose the mechanical energy of one segment into all joint components of causal muscular work. The IPA is useful in determining overall contribution of muscle work to the mechanical energy of all segments, identifying the factor for energy distribution. However, based on our literature review, few studies have applied the IPA to determine the underlying mechanism of the P-D sequential energy flow in baseball pitching and evaluated the multi-joint motor control change over time. Our previous approach, which employed the IPA to investigate collegiate baseball pitching, divided roughly pitching cycle into two primary periods (arm cocking and acceleration phases), and the time-varying motor

control used to achieve the P-D sequential energy flow between the trunk and upper-limb segments is not fully understood.

To attain a detailed understanding of multi-joint control, this study aims to identify the energy distribution mechanism among the segments and determine the effect of the P-D sequence on the mechanical efficiency of the throwing movement, focusing on time-varying motor control. We hypothesize the following: (1) the use of the P-D sequential motion contributes to maximizing the terminal segment kinetic energy (KE) without excessive muscle work of the arm joints, and increases the movement efficiency. (2) Joint control of the sequential motion is consistent with the LJH, in which the proximal joints generate energy for the entire limb motion and distal joints play a role in imparting this energy to the terminal segment. To test the hypotheses, our study divided the pitching cycle into four phases according to the occurrence of peak KEs in each segment, and identified the contributions of the muscular and interactive torques to the mechanical energy distribution during each phase.

2. Materials and Methods

2.1 Experiment

Sixteen male collegiate baseball pitchers (mean ± SD: height 1.78 ± 0.04 m; body mass 78.0 ± 4.6 kg; age 19.3 ± 0.5 years) volunteered to participate in this study. They played for teams

ranked in the first division of the New *Tokyo* University Baseball League or the Tokyo Metropolitan Area University Baseball League, both of which belong to the All Japan University Baseball Federation. No injuries were reported during the study, and the volunteers had no shoulder or elbow surgeries in the year prior to the study. They were all right-handed throwers and had been pitching on competitive youth, high school, and/or collegiate baseball teams for at least eight years. The experimental procedure was explained to the participants, who submitted written informed consent before the trials. The experimental procedure was approved by the Ethical Committee of the Japan Institute of Sports Sciences. After performing a preparation routine of stretching and warm-up throwing, the participants were instructed to throw maximum-effort pitches. Each pitcher threw at least 15 fastball pitches from an indoor pitching mound to a catcher positioned at the regulation distance of 18.4 m from the pitching rubber. The balls and strikes were judged by the catcher. The linear ball velocities of the trials were measured by a radar gun (CR-1K, Toa Sports Machine, Inc., Osaka, Japan) located approximately 1 m behind the catcher. Using subjective criteria, the pitchers ranked their pitches that passed through the strike zone. Based on throws with the greatest velocities measured by the radar gun that had the highest pitcher ratings, five pitches per participant were selected for the analysis. The protocols to instruct the participants to throw maximum-effort pitches and collect the highest-rated pitches were based on a method presented in a previous study (Naito et al., 2017).

A three-dimensional (3D) motion capture system (Vicon MX, Vicon Motion Systems, Oxford, UK) was used to measure the movement via 18 infrared cameras to track the reflective markers attached to the participants at a rate of 250 Hz. In order to estimate the joint center locations and joint coordinate systems, the reflective markers were attached bilaterally at the greater trochanters, lower ends of the ribs, lateral tips of the acromion processes, medial and lateral humeral epicondyles, radial and ulnar styloid processes, and distal end of third metacarpal and fingertip, in accordance with the definition used in a previous study (Naito et al., 2017). Two additional reflective markers, placed on the medial and lateral malleolus of the left leg, were used to identify the stride foot contact (SFC) time, as defined in previous studies (Urbin MA et al., 2013, Naito et al., 2017).

The 3D positional data obtained from the measurement were digitally filtered independently in the X, Y, and Z directions with an 8 Hz Butterworth low-pass filter to calculate the kinematic and kinetic variables. The cut-off frequency of the filter was determined using residual analysis (Winter, 2009). The positional data collected from the moment of contact of the landing foot until ball release were input into the model analysis.

2.2 Throwing system

The throwing model comprised eight rigid segments (1: trunk, 2: scapula, 3: right upper-arm, 4: right forearm, 5: right hand, and 6–8: left upper-arm, forearm, and hand, respectively) and joints with eighteen degrees of freedom (DOF). The four-DOF joints of the trunk and scapula consisted of the trunk backward/forward tilt (J_1), right/left tilt (J_2), counter-clockwise (forward)/clockwise (backward) rotation (J_3), and scapula right/left tilt (J_4). The seven-DOF joints of the throwing arm included shoulder external/internal rotation (J_5), adduction/abduction (J_6), horizontal adduction/abduction (J_7), elbow extension/flexion (J_8), forearm supination/pronation (J_9), wrist extension/flexion (J_{10}), and ulnar/radial deviation (J_{11}). The non-throwing arm joints with seven DOF (J_{12}–J_{18}) correspond to those of the throwing arm. The local reference frames attached to each segment and joint angle (θ_k ; k = 1–18) were determined using the same method previously developed for the analysis of an 18-DOF throwing system (Naito et al., 2011). For the coordinate system, the distal interphalangeal joint of the middle finger was defined as a fingertip, and the location of the ball was assumed to be coincident with that of the fingertip of the throwing hand. The throwing hand fingertip and the proximal point of the trunk were defined as the distal and proximal endpoints of the system, respectively. Kinematic variables were calculated using the recorded positional data obtained from the trials. For the calculation of the kinematic variables, the linear velocities and accelerations of the segments were calculated by assuming the segments as rigid bodies. The forces acting on the

segments and joint torques were computed using the calculated kinematic variables and inverse dynamics. The joint torques were defined as the muscular torques of the joints. Each force and torque were calculated, progressing from the distal to proximal components (segments/joints). The definitions and calculations of joint kinematics and kinetics have been presented in detail previously (Naito et al., 2011, Naito et al., 2018).

The joint force acting at the proximal point of the most proximal-base segment (trunk) was defined as the external joint force acting at the proximal endpoint of the system. According to the calculation and definition from the previous study (Naito et al., 2018), this force was assumed to be provided by the leg joints to support the upper body parts of the system. As the focus was on the upper-body kinetic chain, this study assumed that the external joint force component represents the total effect of all leg joint torque components, instead of analyzing the individual leg joint components. We also defined the muscular joint torque as a residual torque that represents the sum of the torque generated both by contractile activity of the muscles surrounding the joint and by structural viscoelastic properties of the tissue associated with the joint (from the muscles, tendons, ligaments, articular capsule, and other connective tissue). The present study defined the power (work) provided by the muscular torque as the net power or internal power (work), and that of the external joint force was defined as the external joint force power or external power (work). Net power was calculated as the scalar product of the vectors of the muscular torque and angular velocity of the joints. Using the obtained kinematic and

kinetic variables, an IPA was applied to the throwing movements of our participants, as described in the following section.

2.3 Muscular torque power and external joint force power applied to the system

This study used two main equations. One was a free-body equation, and the other was a state-space equation. The state-space equation for a multi-joint kinetic chain system developed in previous studies (Naito et al., 2011; Naito et al., 2018), which is defined as an induced-power equation, was used to decompose the system's mechanical energy into the elements attributed to 'net' power and external joint force power.

For expressing the system using free-body Eqns 1 and 2, the rate of change of the kinetic (KP_i) and potential energies of individual segment i (PP_i) can be decomposed as follows.

$$KP_i = \frac{dKE_i}{dt} = \boldsymbol{v}_{Gi} \cdot m_i \boldsymbol{a}_{Gi} + \boldsymbol{\omega}_i \cdot \boldsymbol{n}_{Gi} = \boldsymbol{v}_p \cdot m_i \boldsymbol{a}_{Gi} + \boldsymbol{v}_{Gi-p} \cdot m_i \boldsymbol{a}_{Gi} + \boldsymbol{\omega}_i \cdot \boldsymbol{n}_{Gi} \quad (1)$$

$$PP_i = \frac{dPE_i}{dt} = \boldsymbol{v}_{Gi} \cdot (-m_i \boldsymbol{g}) = -\boldsymbol{v}_p \cdot m_i \boldsymbol{g} - \boldsymbol{v}_{Gi-p} \cdot m_i \boldsymbol{g} \quad (2)$$

Here, KE_i and PE_i are the kinetic and potential energies of individual segment i, respectively. the rate of change of the segmental kinetic energy (dKE_i/dt) can be decomposed into a component owing to the segmental acceleration about the proximal endpoint ($\boldsymbol{v}_{Gi-p} \cdot m_i\boldsymbol{a}_{Gi} + \boldsymbol{\omega}_i \cdot \boldsymbol{n}_{Gi}$) and that associated with the velocity of the proximal endpoint ($\boldsymbol{v}_p \cdot m_i\boldsymbol{a}_{Gi}$). The rate of change of the segmental potential energy (dPE_i/dt) can be decomposed into a component owing to the segmental translation in the vertical direction relative to the proximal endpoint ($-\boldsymbol{v}_{Gi-p} \cdot m_i\boldsymbol{g}$) and that associated with the velocity of the proximal endpoint ($-\boldsymbol{v}_p \cdot m_i\boldsymbol{g}$). As shown in the above equations, the segmental kinetic and potential energies can be decomposed into a component owing to the segmental acceleration (rotation) around the proximal endpoint of the link system and that associated with the velocity of the proximal endpoint. According to our previous work (Naito et al., 2011; Naito et al., 2018), the current analysis defined that the kinetic and potential energies owing to the segmental rotation around the proximal endpoint of the system are provided by the net power, and those associated with the proximal endpoint velocity are provided by the external joint force power.

Let us first consider the contribution of the net power. The muscular torques provide segmental accelerations about the proximal endpoint; therefore, the net power can be represented as follows.

$$\boldsymbol{T}^T \cdot \dot{\boldsymbol{\theta}} = \sum_{k=1}^{18} T_k\,\dot{\theta}_k = \sum_{i=1}^{7}\left(\boldsymbol{v}_{Gi-p} \cdot \boldsymbol{f}_{Gi} + \boldsymbol{\omega}_i \cdot \boldsymbol{n}_{Gi}\right) + \boldsymbol{v}_{d-p} \cdot \boldsymbol{f}_d \quad (3)$$

$$= \sum_{i=1}^{7} \left(\boldsymbol{v}_{Gi-p} \cdot m_i \boldsymbol{a}_{Gi} + \boldsymbol{\omega}_i \cdot \boldsymbol{n}_{Gi} \right) + \sum_{i=1}^{7} \boldsymbol{v}_{Gi-p} \cdot (-m_i \boldsymbol{g}) + \boldsymbol{v}_{d-p} \cdot \boldsymbol{f}_d \tag{4}$$

The left side of Eqn 3 includes the net power ($\boldsymbol{T}^T \cdot \dot{\boldsymbol{\theta}}$). The right side of Eqn 4 is the summation of the translational ($\boldsymbol{v}_{Gi-p} \cdot m_i \boldsymbol{a}_{Gi}$) and rotational kinetic energies- ($\boldsymbol{\omega}_i \cdot \boldsymbol{n}_{Gi}$), potential energy-related components ($-\boldsymbol{v}_{Gi-p} \cdot m_i \boldsymbol{g}$), and the mechanical (external) power applied to the external object (ball) ($\boldsymbol{v}_{d-p} \cdot \boldsymbol{f}_d$).

With a closed-form state-space power approach, Eqn 4 can also be rewritten as follows:

$$\boldsymbol{T}^T \cdot \dot{\boldsymbol{\theta}} = \sum_{i=1}^{7} \left(\boldsymbol{H}_i \ddot{\boldsymbol{\theta}} + \boldsymbol{R}_i \dot{\boldsymbol{\theta}} + \boldsymbol{V}_i \dot{\boldsymbol{\theta}} + \boldsymbol{C}_i \dot{\boldsymbol{\theta}} + \boldsymbol{G}_i + \boldsymbol{P}_i + \boldsymbol{F}_i \right)^T \dot{\boldsymbol{\theta}}, \tag{5}$$

where $\boldsymbol{H}_i$ is an inertia matrix; $\boldsymbol{R}_i$, $\boldsymbol{V}_i$, and $\boldsymbol{C}_i$ are the angular velocity-dependent terms owing to gyroscopic angular acceleration, Coriolis force, and centrifugal force, respectively, and $\boldsymbol{G}_i$, $\boldsymbol{P}_i$, and $\boldsymbol{F}_i$ are the torques owing to gravity, linear acceleration of the proximal endpoint, and external force applied to the ball, respectively. The definition of each term corresponds to that presented in previous studies (Naito et al., 2011; Naito et al., 2018). In Eqn 5, the motion-dependent terms express the change in

kinetic energy, and the gravity-dependent term is the change in potential energy of the system. The external force-dependent term is the mechanical power applied to the ball. Each dependent term can be described as follows.

$$\left(\boldsymbol{H}_i\ddot{\boldsymbol{\theta}} + \boldsymbol{R}_i\dot{\boldsymbol{\theta}} + \boldsymbol{V}_i\dot{\boldsymbol{\theta}} + \boldsymbol{C}_i\dot{\boldsymbol{\theta}} + \boldsymbol{P}_i\right)^T\dot{\boldsymbol{\theta}} = \boldsymbol{v}_{Gi-p} \cdot m_i\boldsymbol{a}_{Gi} + \boldsymbol{\omega}_i \cdot \boldsymbol{n}_{Gi} \tag{6}$$

$$\boldsymbol{G}_i{}^T \cdot \dot{\boldsymbol{\theta}} = \boldsymbol{v}_{Gi-p} \cdot (-m_i\boldsymbol{g}) \tag{7}$$

$$\boldsymbol{F}_i{}^T \cdot \dot{\boldsymbol{\theta}} = \boldsymbol{v}_{d-p} \cdot \boldsymbol{f}_d \tag{8}$$

Next, we will define the contribution of the external joint force component to the system. As the external joint force acting on the most proximal-base segment (trunk) affects the accelerations of the upper body parts, the joint force acting at the proximal endpoint ($\boldsymbol{f}_p$) and the force power ($\boldsymbol{v}_p \cdot \boldsymbol{f}_p$) can be represented as follows.

$$\boldsymbol{f}_p = \sum_{i=1}^{7} m_i\boldsymbol{a}_{Gi} - \sum_{i=1}^{7} m_i\boldsymbol{g} + \boldsymbol{f}_d \tag{9}$$

$$\boldsymbol{v}_p \cdot \boldsymbol{f}_p = \sum_{i=1}^{7} \boldsymbol{v}_p \cdot m_i \boldsymbol{a}_{Gi} - \sum_{i=1}^{7} \boldsymbol{v}_p \cdot m_i \boldsymbol{g} + \boldsymbol{v}_p \cdot \boldsymbol{f}_d \tag{10}$$

As shown in Eqn 10, the external joint force-related power ($\boldsymbol{v}_p \cdot \boldsymbol{f}_p$) is divided into the changes in kinetic and potential energy of the system segments and mechanical energy applied to the ball associated with the velocity at the proximal endpoint ($\boldsymbol{v}_p$).

The total kinetic energy change of individual segment i (KP_i), which is equal to the sum of the net power- (KP_{Ni}) and external joint force power-related components (KP_{Ji}), can be expressed as follows.

$$KP_i = KP_{Ni} + KP_{Ji}, \tag{11}$$

where

$$KP_{Ni} = KP_{Ti} + KP_{Ri} + KP_{Vi} + KP_{Ci} + KP_{Gi} + KP_{Pi} + KP_{Fi}$$

The following are the net power-related components.

Muscular torque-induced power: $KP_{Ti} = \left(\boldsymbol{H}_i \ddot{\boldsymbol{\theta}}_T\right)^T \dot{\boldsymbol{\theta}}$

Gyroscopic moment-induced power: $KP_{Ri} = \left(\boldsymbol{H}_i \ddot{\boldsymbol{\theta}}_R + \boldsymbol{R}_i \dot{\boldsymbol{\theta}}\right)^T \dot{\boldsymbol{\theta}}$

Coriolis force-induced power: $KP_{Vi} = \left(\boldsymbol{H}_i \ddot{\boldsymbol{\theta}}_V + \boldsymbol{V}_i \dot{\boldsymbol{\theta}}\right)^T \dot{\boldsymbol{\theta}}$

Centrifugal force-induced power: $KP_{Ci} = \left(\boldsymbol{H}_i \ddot{\boldsymbol{\theta}}_C + \boldsymbol{C}_i \dot{\boldsymbol{\theta}}\right)^T \dot{\boldsymbol{\theta}}$

Gravity-induced power: $KP_{Gi} = \left(\boldsymbol{H}_i \ddot{\boldsymbol{\theta}}_G\right)^T \dot{\boldsymbol{\theta}}$

Trunk linear acceleration-induced power: $KP_{Pi} = \left(\boldsymbol{H}_i \ddot{\boldsymbol{\theta}}_P + \boldsymbol{P}_i\right)^T \dot{\boldsymbol{\theta}}$

External force-induced power: $KP_{Fi} = \left(\boldsymbol{H}_i \ddot{\boldsymbol{\theta}}_F\right)^T \dot{\boldsymbol{\theta}}$

Here, $\ddot{\boldsymbol{\theta}}_T$, $\ddot{\boldsymbol{\theta}}_R$, $\ddot{\boldsymbol{\theta}}_V$, $\ddot{\boldsymbol{\theta}}_C$, $\ddot{\boldsymbol{\theta}}_G$, $\ddot{\boldsymbol{\theta}}_P$, and $\ddot{\boldsymbol{\theta}}_F$ denote the joint angular accelerations induced by the muscular torque, gyroscopic moment, Coriolis and centrifugal forces, gravity, trunk linear acceleration, and external force, respectively.

The external joint force power-related component is as follows.

$$KP_{Ji} = \boldsymbol{v}_p \cdot m_i \boldsymbol{a}_{Gi} \tag{12}$$

The total potential energy change of an individual segment i can be expressed as shown below.

$$PP_i = PP_{Gi} + PP_{Ji} \tag{13}$$

where

$PP_{Gi} = \boldsymbol{G}_i{}^T \dot{\boldsymbol{\theta}}$

$PP_{Ji} = \boldsymbol{v}_p \cdot (-m_i \boldsymbol{g})$

From Eqn 13, the total potential energy change of the segment (PP_i) can be decomposed into the net power- (PP_{Gi}) and external joint force power-related components (PP_{Ji}).

The total mechanical (external) power applied to the ball (EP_{ball}), which is determined by the net power- and external joint force power-related components, is represented as follows.

$$EP_{ball} = \boldsymbol{v}_p \cdot \boldsymbol{f}_d + \boldsymbol{v}_{d-p} \cdot \boldsymbol{f}_d \tag{14}$$

Using Eqns 1-14, the relationship between the energy sources (net power and external joint force power) and distributed energy (changes in the segmental kinetic and potential energies and mechanical power applied to the ball) in the overall system can be rewritten as follows.

$$\boldsymbol{T}^T \cdot \dot{\boldsymbol{\theta}} + \boldsymbol{v}_p \cdot \boldsymbol{f}_p = \sum_{i=1}^{7} (KP_i + PP_i) + EP_{ball} \tag{15}$$

The first and second terms on the left side of the equation indicate the net and external joint force power, which are defined as the energy sources. The right side of the equation indicates the energy distributed to the segments.

Regarding the muscular joint torque, we also consider that the net power can be separated into the power applied to the system segments and power applied to the ball. The overall contribution of the net power to the system can be rewritten as shown below.

$$\boldsymbol{T}^T \cdot \dot{\boldsymbol{\theta}} = \sum_{k=1}^{18} T_k \, \dot{\theta}_k = INT_{kinetic} + INT_{potential} + EXT \tag{16}$$

where

$$INT_{kinetic} = \sum_{i=1}^{7} KP_{Ti} + KP_{Ri} + KP_{Vi} + KP_{Ci} + KP_{Gi} + KP_{Pi} + KP_{Fi}$$

$$INT_{potential} = \sum_{i=1}^{7} PP_{Gi}$$

$$EXT = \boldsymbol{f}_{d-p} \cdot \boldsymbol{f}_d$$

Eqn 16 shows that the net power is expended on the internal power related to the changes in the kinetic ($INT_{kinetic}$) and potential energy ($INT_{potential}$) of the segments and external force-related power applied to the ball (EXT).

The validity of the present analysis was confirmed by comparing between the mechanical energy calculated by the free-body equations (Eqns 1 and 2) and that obtained by the integral of each component included in Eqns 11-13, as presented in our previous studies (Naito et al., 2011; Naito et al., 2018).

2.4 Assessment of each factor-induced component

The measured pitching movement cycle was separated into four phases. The period between the SFC and maximum trunk KE, that between the maximum KE of the trunk and upper-arm, that between the upper-arm and forearm, and that between the forearm and hand were defined as phases 1–4, respectively. The causal torque component contribution to determine the system's mechanical power was obtained using the following method. First, the kinematic and kinetic variables obtained from the recorded trials were inputted into the state-space power equations. Second, each power component computed by the induced-power equation was integrated forward in time during a specific phase. From these two processes, the work-energy relationships between the causal energy sources and distributed mechanical energies were evaluated. The kinetic and potential energy of the system segments were decomposed into various force- and torque-induced components. The work performed by the individual joint torque (internal work) and external joint force (external work) was decomposed into the components of work expended on the kinetic and potential energies of each segment.

Kinematic analyses generally adopt the kinematic variables of particular joints to assess the subject performance. Based on previous studies (Van den Tillaar and Ettema, 2009; Reid et al., 2015), the maximum angular velocities of trunk forward rotation, shoulder internal rotation, shoulder horizontal adduction, and elbow extension were assessed. Specific temporal events in the pitching cycle, including the distinctive kinematic parameters and occurrence of maximum KEs of each segment, were normalized as percentage values of the SFC for ball release (REL). For the normalized time, the instants of SFC and REL were defined as 0% and 100%, respectively. Thus, when an event occurred after REL, the normalized time of that event was indicated as greater than 100%.

2.5 Assumption and interpretation of each factor

This study assumed that the mechanical energy cause of the segment (energy source) is exerted by the joint torque work owing to muscle concentric and eccentric contractions. We also assumed that the intersegmental joint forces and torques, which are defined as muscular torque and motion-, gravity-, and external force-dependent torques in our analysis, redistribute the energy between different segments and do not change (increase/decrease) the level of the mechanical energy of the entire system. Based on these definitions, it is assumed that even if passive torques (e.g. gravity-dependent torque) act between different segments, they would

compensate each other, and the total mechanical energy of the entire system would not change unless muscular torques apply their power to the system.

A previous analysis that examined seated ergometer pedaling (Fregly and Zajac, 1996) categorized the mechanical energy flow into 12 types, and the effects of the muscular joint torque on the system dynamics were divided into three primary influences: energy generation, absorption, and transfer. Using this categorization in this study, the joint torque function is defined as follows. When the muscular joint torque generates positive power (work) and that power (work) is exploited to increase the mechanical energy of a system segment, the function of the muscular joint torque is defined as an energy source. When the muscular joint torque or intersegmental joint force accelerates a limb segment while simultaneously decelerating other segments without work generation of the joint torque (force), that joint torque/force transfers the mechanical energy from the decelerated segment to the accelerated one. The role of the muscular joint torque on the energy transfer between the different segments is defined as an energy channel. For example, shoulder joint torque acting to accelerate the humerus (a distal segment) and decelerate the trunk (a proximal segment), transferring mechanical energy out of the proximal segment into the distal one, functions as the energy channel. For an ideal case of the energy channel, in which the limb motion depends only on the energy transfer mechanism, the joint torque power consumption for moving the limb would be zero.

In a multi-joint-link system, a joint torque acting to accelerate the segment instantaneously results in the acceleration of all other segments on which its torque does not act, because of the intersegmental dynamics (Zajac et al., 2002). To comprehensively understand the cause of mechanical energy, the present analysis evaluated the overall contribution of the muscle work of the individual joints to the mechanical energy of all components (segments and ball) during the respective and overall phases.

The function of the proximal trunk joints as an energy source for driving the distal arm segments is the focus of this study. It should be noted that the contribution of the trunk joint work to the arm segment KE represents the work except for the component expended for the trunk acceleration. Thus, the relatively great mass of trunk segment does not significantly influence our interpretation of the contribution of the trunk joint to the cause of the arm segment KE.

2.6 Control indices

The trunk and throwing upper-arm, forearm, and hand were defined as the trunk-arm system. Based on the mechanical work-energy principle for a rigid-body system, the change (increase/decrease) in the KE of the entire-system equals the expenditure of the muscle work for this energy change (Zatsiorsky, 2002). As the reduced KE of a segment can instantaneously result in increased KE of the other segments, if the reduced KE could be fully transferred to the

increased KE, positive muscular work would not be expended for increasing the segment KE. Therefore, the energy-increasing characteristics can be identified by evaluating the amount of muscle work expenditure within the trunk-arm system. To assess the cause of the energy increase, we defined two different factors. First, when the increase in the energy of some segments depended on muscle work production, the energy increase was defined as *energy-generation*. Second, when the increase in energy was caused by KE exchange between the accelerated and decelerated segments without work production, the energy increase was defined as *energy-transfer*.

For the trunk-arm system, the relationship between the increased/decreased KE of each segment and total work expended for the change of the KE can be described as follows.

$$total\ work = segment\ KE^{+} + segment\ KE^{-} \tag{17}$$

Here, *segment* KE^{+} is the sum of the increased segment KE, and *segment* KE^{-} is the sum of the decreased segment KE for a specific phase. *Total work* is defined as the sum of the work done by the individual joint during the same phase.

Using Eqn 17, the *segment* KE^{+} can be calculated using the *total work* and *segment* KE^{-} terms, as follows.

$$\frac{segment\ KE^{+}}{segment\ KE^{+}} = \frac{total\ work}{segment\ KE^{+}} - \frac{segment\ KE^{-}}{segment\ KE^{+}} \quad (18)$$

The first (*total work* per *segment KE*$^{+}$) and second terms (*segment KE*$^{-}$ per *segment KE*$^{+}$) on the right side of the equation were defined as an *energy-generation* and *energy-transfer* factors, respectively. As defined in the equation, these two factors represent the relative contribution (%) to the sum of increased KE of certain segments during a specific phase. The sum of both factors equals 100%. We defined these factors as the control indices (CI). The CI were used to evaluate which factor predominantly contributed to the energy increase and by how much. For example, when an energy-transfer factor accounts for 100%, we interpret that the energy increase is the result of energy transfer with no work done.

3. Results

3.1. Normalized time and maximum values of kinematics, kinetics, and mechanical energy

The mean linear ball velocity measured by the radar gun was 36.2±1.4 m/s (130.3± 5.0 km/h). The mean resultant fingertip velocity at ball release calculated by the rigid-body model was 32.8 ± 2.3 m/s. In all trials, the maximum value of the resultant fingertip velocity occurred at the time of ball release.

For the mean maximum angular velocity (Table 1), the shoulder internal rotation had the greatest value, followed by elbow extension, trunk rotation, and shoulder horizontal adduction. The normalized time showed that the maximum angular velocities of the trunk rotation, shoulder horizontal adduction, and elbow extension were shown as the P-D sequential order (Table 1).

Regarding the change in the mechanical energy in a specific period, the increases of the system mechanical energy and KE of the trunk-arm system were the largest in phase 1 (Fig. 1A). The changes of those energies during phases 2–4 were not relatively large, compared with those in phase 1.

The temporal timing of the maximum KE of the segments was exhibited as a P-D sequential order, indicating that the occurrence of maximum KE of the trunk was followed by that of the upper-arm, forearm, and hand (Figs. 1B and 2B and Table 1). The maximum KE of the hand occurred at the instant of ball release (Table 1). The maximum KE of the trunk was the greatest among the trunk-arm system segments, followed by that of the hand, upper-arm, and forearm (Table 1 and Fig. 1B).

3.2 Contributions of the causal factor-induced components to the change in the segmental KE in each phase

The results of how energy sources are distributed across the segments are presented in this section. The origins of the internal work (energy sources) are presented in the following sections. It should be noted that the energy inflow and outflow between segments changes through the phases (see the following figures in this section).

The change in the KE during the specific phases (net KE in the figures) and the decomposition of the net KE into the muscular and interactive torque-induced components are shown in Figs. 3–6A, C, E, and G. The individual joint contributions of the muscular torque- (MUS), Coriolis force- (COR), and centrifugal force- (CEN) induced components to the net KE are shown in Figs. 3–6B, D, F, and H. The relative contribution of the energy-generation/transfer of control index is shown in Figs. 3–6.

In phase 1 (Fig. 3), the increase in the net trunk KE was 218.2±8.0 J. This value was the greatest magnitude among all components of the system segment KE during all phases. This magnitude of the trunk KE was induced primarily by the external joint force- and MUS-induced components. In MUS, the trunk backward/forward tilt (J_1) was the greatest, and the trunk counter-clockwise/clockwise rotation (J_3) was greater than that of the other joint positive components (Fig. 3B). The increases in the net KE of the upper-arm, forearm, and hand were less than that of the trunk.

In phase 2 (Fig. 4), the net KE of the upper-arm, forearm, and hand increased, while that of the trunk decreased. The MUS-induced components of the upper-arm (76.3 J) and forearm (62.6 J) had the largest positive contribution to the increased KEs, accounting for more than 97% of the internal work on the upper-arm (78.5 J) and forearm (62.0 J), while the MUS-induced component produced negative effect on the trunk. The decrease in the net trunk KE was primarily attributed to the negative contributions of the external joint force- and MUS-induced components. For the individual joint contributions, the shoulder horizontal adduction/abduction (J_7) in MUS had the largest positive contributions to the KE of the upper-arm and forearm, while this joint contribution to the KE of the trunk had the largest negative contribution among all components (Fig. 4B, D, and F).

In phase 3 (Fig. 5), the net KE of the forearm and hand increased, while those of the upper-arm and trunk decreased. The MUS-induced components had the largest positive contributions to the forearm and upper-arm, while this component had the largest negative contribution to the trunk KE. The CEN-induced component had the largest positive contribution to the hand, while this component had the largest negative contributions to the upper-arm and forearm KEs. The shoulder horizontal adduction/abduction (J_7) in MUS had the largest positive contribution to the increased KE of the forearm and upper-arm (Fig. 5D and F).

In phase 4 (Fig. 6), the net KE of the hand increased, while that of the trunk, upper-arm, and forearm decreased. The increased KE of the hand was attributed to the positive contributions of the CEN-, MUS-, and COR-induced components. The CEN-induced component had the largest positive contribution to the hand, while that component had the largest negative contribution to the upper-arm and forearm (Fig.6C, E, and G). The MUS-induced components increased the KE of the upper-arm, forearm, and hand in this phase. The elbow extension/flexion (J_8) in CEN had the largest effect on increasing the hand KE and reducing the upper-arm KE. The shoulder external/internal rotation (J_5) in MUS had a larger effect on increasing the KE of the hand, forearm, and upper-arm than that of other components (Fig. 6D, F and H).

As shown in the CI of Figs. 3-6, in phase 1, the energy-generation accounted for 100.0% of the energy increase. In phases 2 and 3, the energy-transfer accounted for 61.3% and 67.2%, respectively. The energy-transfer accounted for 100.0% in phase 4.

3.3 Contributions of the joint work to the segment KE in each phase

The decomposition of the causal internal work resulting in the change of the net segmental KE into individual joint contributions is shown in Fig. 7. The muscle work of the trunk and shoulder joints had a large influence on the change in the segment KE in all phases.

The internal work applied to the trunk in phase 1 (97.8±16.5 J) was primarily exerted by the trunk backward/forward tilt (J_1) and counter-clockwise/clockwise rotation components (J_3) (Fig.

7A). The largest contribution to the internal work applied to the upper-arm in phase 2 was attributed to the trunk right/left tilt (J_2), followed by the trunk counter-clockwise/clockwise rotation (J_3) (Fig. 7B). The trunk backward/forward tilt (J_1) and counter-clockwise/clockwise rotation (J_3) contributions to the forearm were larger than those of the other joints in phase 3 (Fig. 7C). In phase 4, the trunk counter-clockwise/clockwise rotation (J_3), backward/forward tilt (J_1), and shoulder external/internal rotation (J_5) accounted for the major portion of the work exerted on the hand (82.0±15.5 J) (Fig. 7D).

3.4 Muscle work output during the phase

Regarding the total muscle work in each phase, which corresponds to the sum of all joint contributions, the work in phase 1 (198.1±10.8 J) was the greatest value among those of all phases (Fig. 8). Regarding the generated work in phase 1, the trunk counter-clockwise/clockwise rotation (J_3) was the greatest, followed by the trunk backward/forward tilt (J_1) and right/left tilt (J_2). After phase 1, the total muscle work generated in the specific periods reduced over time. The total muscle work generated in phases 2, 3, and 4 were 63.9 J, 45.6 J, and 21.4 J, respectively. In phases 2 and 3, the trunk backward/forward tilt (J_1) generated a significant amount of work (76.0 J and 39.1 J, respectively), and the trunk counter-clockwise/clockwise rotation (J_3) were greater than those of the other joint components in the same phases. In phase 4, the shoulder external/internal rotation (J_5) performed the most work.

3.5 Total contributions of the muscular joint work to the entire system

The relationships between the individual joint work and work expenditure on the system mechanical energy throughout the overall pitching phase, which is obtained by Eqn 16, are listed in Table 2. The sum of the total muscle work performed by all individual joints, responsible for the overall internal work expended on the entire system, was 329.2 J. The work expenditure on the hand KE and ball mechanical energy (hand:167.2 J + ball:72.1 J) accounts for approximately 72.7% of the overall total internal work (329.2 J). The work performed by the trunk backward/forward tilt (J_1) (hand:92.6 J and ball:35.4 J) and counter-clockwise/clockwise rotation joints (J_3) (hand:84.0 J and ball:33.3 J) were the primary energy sources of the mechanical energy of the hand (167.2 J) and ball (72.1 J). These two joint contributions (92.6 J plus 84.0 J) accounted for approximately 95% of the KE of the hand (167.2 J). The total contributions of the shoulder external/internal rotation joint work (J_5) to the hand KE (9.8 J) and ball mechanical energy (5.1 J) were not relatively large, compared with those of the trunk joints. The elbow extension/flexion (J_8) had a negative effect on the hand (-19.0 J) and ball (-1.5 J).

4. Discussion

4.1 Motor control strategies exploited in different stages

The multi-articulated nature of the human body generally has a high redundancy of joint DOFs, and movement can be organized in many ways. For example, the joints could be accelerated simultaneously. The fact that the P-D sequence is observed in human motions indicates that the CNS selects a specific control strategy that results in this sequence. We consider that the energy flow perspective provides key insight for understanding the control strategy. The purpose of this study is to determine the energy distribution mechanisms of baseball pitching and evaluate the effect of the P-D sequence on the movement efficiency, focusing on the motor control strategy. Our hypotheses were that the P-D sequential motion could contribute to efficient throwing, and this motion pattern could be consistent with the theory of the LJH. Our analysis supports previous theories and provides new insight on the control strategy of multi-joint limb coordination, as discussed below.

The current results (see Section 3.1) demonstrated that the peak KEs of the trunk, throwing upper-arm, forearm, and hand segments appeared in the P-D sequential order. The joint control for delivering energy between the system segments changed over time, and the movement strategy could be divided into three stages.

The first stage is building the KE of the trunk during the early period of movement. This energy increase is required to provide the energy source necessary for the consequent arm acceleration that occurs in the following period. The results of phase 1 demonstrate this mechanism. A large amount of the trunk KE was exerted by the work of the external joint force and trunk muscle joint torques (Fig. 3). The increase in the system KE in phase 1 was greater than that in the other phases, and it was caused by the energy-generation factor, as shown in the CI. The trunk segment is the most proximal segment in our model and is more massive than each segment of the upper-extremity; therefore, the KE increase of the trunk is advantageous for obtaining a high level of energy and limiting the muscle work required of the distal arm joints for driving the upper-limb in the late phase.

In the second stage, the energy distribution mechanism from the proximal-to-distal segments is caused by the cooperation of two joints, one acting as an energy source and one as a channel). The results of phases 2 and 3 represent the use of this mechanism. In phases 2 and 3, the KE of the throwing upper-arm and forearm increased depending on the shoulder horizontal adduction (HAD) muscular torque, while this torque was the most dominant factor for the reduced trunk KE in the same phase (Figs. 4 and 5). Therefore, the shoulder HAD muscular torque acted as an energy channel for transferring energy out of the trunk into the upper arm-forearm. The existing energy of the trunk increased before phase 2, and the joint work of the trunk muscles generated

in phases 2 and 3 served as an energy source. Thus, the trunk muscular joint work generated in phase 1 played a significant role in the energy source for increasing the KE of the upper-extremity, whereas the shoulder HAD muscular torque acted as an energy channel that redistributed the mechanical energy between the segments.

The final stage includes maximizing the KE of the hand in phase 4. In this phase, the increase in the hand KE and decrease in the upper arm-forearm KE were attributed to the CEN-induced components and the elbow extension/flexion joint component depending on the centrifugal force, resulting in the energy exchange between the proximal and distal segments. Thus, the elbow extension motion owing to passive interaction torque acted as the energy channel transferring energy from the proximal (e.g., humerus) to the distal segments (e.g., hand). These results are consistent with previous findings of the induced-acceleration analysis that passive angular velocity-dependent torque results in rapid elbow extension before ball release (Hirashima et al., 2008) and our previous work (Naito et al., 2011). Our analysis also suggests that the main role of the elbow joint in this phase is the energy channel, which induces energy transfer from the upper arm-forearm to the hand. The CI indicated that the energy distribution in phase 4 resulted completely from the energy-transfer factor (Fig. 6). Thus, how the elbow joint acts as the energy channel may be key factor in the energy supply to the distal hand. While the centrifugal force-induced elbow extension functions

as the energy channel, the negative effect of the elbow extensor/flexor-dependent component is shown in Table 2. The negative effect of the elbow muscular torque, which acts to reduce the KE of the forearm (-30.1 J) and hand (-19.7 J), represents the energy sink. The negative effect of the elbow flexion torque occurring before ball release has been reported in other studies (Hirashima et al., 2008; Naito and Maruyama, 2008), and is explained by the compensation mechanism for adjusting the timing of ball release (Hirashima et al., 2003). Because of its relatively less contribution, the effect of the energy sink of the elbow was irrelevant to the P-D sequence.

The current findings described above imply that the control strategy for organizing the factors has at least two characteristics. First, the primary energy source of the entire-system was provided by the massive proximal joints (trunk and leg muscles), and this energy was provided in the early stage. The increase in the system KE after phase 1 was not large. Second, the functional roles of the joints changed over time. The shoulder HAD muscular torque in phase 2 and elbow extension joint motion in phase 4 acted as the energy channel, transferring energy from a proximal segment to a distal one. Therefore, the movement strategy of the throwing system requires joint control to redistribute the energy from the proximal segments to the distal segments under a limited amount of energy source. The role of the motion generator (role of the joint as the energy channel) switched from the shoulder to the elbow, and the energy source switched from the KE of the proximal segment (trunk) to that of the distal one (upper-limb) as

the pitching movement cycle proceeded. Thus, if different segments in the linked chain of the arm accelerate simultaneously, far from the P-D sequential energy flow, the energy cost for the driving arm would be imposed on the throwing-arm joints. We conclude that the P-D sequential motion is an effective strategy to utilize the massive trunk and leg muscles as energy sources for increasing the hand KE and reducing the muscular work production of the arm joints. These findings support our hypothesis that the use of the P-D sequence assists in efficient throwing. From the energetic perspective, the current findings also accept the second hypothesis that joint control in fastball throwing is consistent with the LJH theory, in which the proximal joints produce a dynamic foundation of the entire system and distal arm joints utilize the obtained energy to fulfill the task-goal (applying energy to the hand). Previous investigations of multi-joint control for achieving performance accuracy during rapid horizontal arm swing (Kim and Dounskaia, 2009) and overarm throwing at different ball speed (Hirashima et al., 2007) found that skilled performances depend on a control strategy that the leading (proximal) joint motion generates a powerful interaction torque at the other (subordinate) joints, and the distal (subordinate) joint regulates the interaction torque to achieve the task. Their studies imply that this joint control is beneficial for compensating less muscle torque output at the distal joint, while maintaining high-speed of the limb motion. The results of the current analysis agree with their suggestion. Our study suggests that the LJH relates to not only the increase in the rotational speed of the limb but also the reduction in the cost of the work produced by the arm

joints. Investigations of multi-joint arm movements for goal-directed task, such as reaching task (Isableu and Berret, 2016) and throwing at different ball speeds (Hirashima et al., 2003), have found that the skilled movements effectively exploit the interaction torque to achieve the task-goal. In addition to the kinetic account, our energetic approach suggests that the interaction torque plays a crucial role in reducing the mechanical work of the distal arm joints for the arm driving. Mechanical efficiency is the key factor for organizing skilled performances.

Possible reasons for why the joint motion control should change over time can be explained by three factors from biological and mechanical aspects. One factor is derived from the biological property of the muscles. Muscle contraction properties generally depend on a force-velocity relationship, in which muscle force generally reduces depending on the increase in the shortening speed of muscle contraction (Hill, 1938). At the end of the pitching movement cycle, the fast upper-limb joint rotations are required (e.g., rapid elbow extension); however, the muscular torques of the arm joints cannot generate large power, because greater muscular torque is not be compatible with greater joint angular velocity owing to the muscle force-velocity relationship. This analysis showed that the maximum angular velocity of the elbow extension exceeded that of the trunk forward rotation (Table 1), and the supplied energy to the hand at ball release was primarily dependent on the trunk muscle work (Table 2). The control strategy, which employs the shoulder and elbow joints as the energy channel and not as the

primary energy source, can be used to avoid the limiting factor of the force-velocity relationship of muscle contraction.

Another factor relates to the mechanical constraints of the system. The existing energy of the proximal segment serves as the primary energy source, and this energy flows out of the proximal segment to the distal one. The muscle work supplied to the entire-system decreases as the pitching movement cycle progresses. The task-goal of the pitching movement is to deliver more energy to the terminal segment. Therefore, the KE of the proximal segments should be reduced because if some segments could gain more energy, the remainder of the energy applied to the extra segments would be less. Our study predicts that deceleration of a proximal segment (e.g., trunk), in combination with the roles of the joint as an energy channel, would aid effective energy flow from the proximal to the distal segments (e.g., from the trunk to the upper-limb) rather than simultaneously accelerating the trunk and upper-limb segments. Switching the movement generator from the shoulder to the elbow might control this effective energy flow.

In addition to the two factors, the third possible factor is minimization of neural effort (Dounskaia and Shimansky, 2016). This theory hypothesizes that organization of multi-joint control has a tendency to reduce the 'neuro-computational' cost. Our study found that the target segment of the link-system, to which the muscular joint torques apply their power, changed over time, and a time-varying pattern of the target was exhibited as a P-D sequential order. For example, in phase 2, the KE of the entire-arm (upper-arm, forearm, and hand) increased

whereas that of the trunk decreased. In this case, the entire-arm was the target. In phase 3, the KE of the forearm-hand segments increased, whereas that of the upper arm-trunk decreased. In this case, the forearm-hand was the target. In phase 4, as the hand segment only gained KE, the hand was the target. Our study speculates that the CNS might possibly handle some segments as one target segment, by stabilizing some joints. Stabilizing the joints or reducing the number of active (mobile) DOFs might simplify the neuro-effort for joint control, because the complexity of mechanical linkage of multiple joints is reduced.

4.2 *Implications for effective multi-joint movement control*

Fregly and Zajac (1996) found that the cooperation between the proximal hip and distal ankle joints is beneficial for delivering the power generated by the large muscular torque at the hip to the ankle joint applying force to the crank. In their study, the cooperation between the energy source and energy channel to exert force on the target object is defined as synergy. Our study suggests that the trunk (energy source) and shoulder joints (energy channel) may act in synergy, because if these two elements could not function, the trunk KE would not be imparted to the upper-limb. Our study accepts the explanation that exploitation of the synergetic cooperation between different joint functions is an appropriate way to utilize the large amount of joint work by large muscle torques acting at a proximal joint to assist or support the function of the weaker distal joint (Fregly and Zajac, 1996).

The summation of speed principle (Bunn, 1972), which speculates that the system will achieve an optimum endpoint velocity if the distal segment begins its motion at the time of maximum speed of the proximal segment, has been frequently applied as a general explanation of an ideal motion pattern for throwing (e.g., Kreighbaum and Barthels, 1996). However, the summation of speed principle does not provide a mechanical explanation for why the ideal motion pattern is an optimal sequence. Based on our results, the shoulder HAD muscular torque in the second stage acts as the energy channel. Therefore, if the trunk could effectively decelerate by the shoulder HAD torque, more energy would flow from the trunk to the upper-limb. To increase the effectiveness of the energy flow, the KE level of the trunk should be increased before the shoulder HAD torque action and subsequently decreased by the shoulder HAD torque in the second stage. The timing of the initiation of the acceleration and deceleration of the segments could affect successful energy transfer. The acceleration of the upper-arm should be initiated after the trunk segment obtains sufficient KE. Based on these findings, the current study suggests that the theory of the summation of speed principle is associated with effective energy transfer.

Previous analysis found that the rapid elbow extension before the ball release during pitching was induced primarily by the interaction torque depending on the angular velocity of the shoulder HAD and upper trunk forward rotation (Naito and Maruyama, 2008). That study suggested that the shoulder HAD muscular torque generated positive torque to resist and overcome the negative

interaction torque effect that decelerates the HAD motion. The present finding that the shoulder HAD functions as the energy channel is consistent with those previous findings. It is implied that the shoulder HAD needs to generate a positive joint torque to maintain a certain angular velocity for imparting the interaction torque effect to the forearm, and not to produce excessive angular acceleration of the HAD joint.

The previous kinetic comparison showed that the maximum shoulder internal rotation (IR) torque of a higher ball velocity group tends to be greater than that of a lower ball velocity group (Escamilla et al., 2002; Fleisig et al., 1999). Given the positive contribution of the IR work to the arm segments (Table 2), our study agrees with the previous findings that the shoulder internal rotator attempts to produce a high projectile velocity. However, despite the largest work generated in phase 4 (Fig.8 D), the contribution of the IR work to the throwing hand-ball mechanical energy in the overall phase was not relatively large. In addition, the IR torque simultaneously exerted work on the upper-arm, forearm, and hand in phase 4 (Fig. 6). These results likely reflect the action of the shoulder internal rotator simultaneously accelerating the upper-limb segments. Thus, the IR torque does not relate to the P-D sequential energy flow. These facts imply that the IR power is likely important for rapid arm rotation in the late period of the pitching cycle, but the shoulder IR power may not be the determinant factor for the final KE output of the throwing hand. An analysis of the normalized time indicates that the IR motion (i.e. arm-acceleration phase) generally occurs for a short time period, within 20% of the

entire-pitch cycle (Fleisig et al., 1999). The relatively short time period of IR positive power generation probably has an influence on the less amount of total work, which is defined as the time integral of the IR power. The current findings imply that the IR functions as a joint torque component that accelerates the entire-arm and delivers its power to the terminal segment independently, not through sequential joint motions. Also, elastic energy stored at the shoulder muscles is important for producing the rapid IR motion (Roach et al., 2013). Our data suggest that increasing the shoulder IR power, amplified by the elastic energy storage, likely increases the power exerted on the throwing-arm, but this action might not improve the effectiveness of the P-D sequential energy flow and efficiency of throwing.

4.3 Advantage of the current analysis

Recently, Induced-acceleration analyses (IAAs) have been used to examine multi-joint control in rapid upper-limb movements (Hirashima, 2011; Hirashima et al., 2007; Kim and Dounskaia, 2009). However, the interpretations of multi-joint control obtained from our analysis is not completely consistent with those from previous analyses. Conventional IAAs generally recognize motor control behavior by assessing whether the muscular joint active torque acts to assist or resist a passive joint motion resulting from the interaction torque effect. For example, previous studies used a specific index, which was defined using a positive (assistive) or

negative (counteractive) relationship between the muscular and interaction torques, to interpret the control strategy in multi-joint fast limb motions (Hirashima et al., 2003; Kim and Dounskaia, 2009). In this definition, the counteractive relationship between the muscular and interaction torque effects is interpreted as a compensatory effect (Hirashima, et al., 2007). Conversely, in our analysis, the role of a joint torque/motion was interpreted based on its influences on the energy increase of a distant segment and the energy cost of the system. Based on this context, a negative contribution of joint torque (the torque reducing a segment KE, acting as the energy channel) is an essential element for effective energy transfer. As previously discussed, an effective energy transfer may be required to realize a synergetic effect between energy source and channel. Thus, the counteraction of the muscular torque against the interaction torque should not be necessarily explained as a compensatory action to resist or diminish the interaction torque effect. In addition, IAAs do not generally conduct a quantitative assessment of the energy transfer and mechanical efficiency. Our finding is that the joint work generated in the early period was utilized as the energy source for the consequent arm rotation occurring in the later period. Thus, for accurately understanding the movement efficiency, an analysis should take into consideration for assessing how long the system energy is conserved beyond a specific period. Because IAAs, which are not direct approaches for calculating the mechanical energy, do not generally evaluate the energy conservation, the current approach

would be helpful for providing more practical knowledge on efficient movement strategy than the IAAs.

Notations

i: segment number

k: joint number

m_i: mass of i-th segment

$\boldsymbol{g}$: gravity

$\dot{\boldsymbol{\theta}}$: joint angular velocity

$\ddot{\boldsymbol{\theta}}$: joint angular acceleration

$\boldsymbol{v}_{Gi}$: velocity of mass center of i-th segment

$\boldsymbol{a}_{Gi}$: acceleration of mass center of i-th segment

$\boldsymbol{f}_{Gi}$: force acting on i-th segment

$\boldsymbol{v}_{Gi-p}$: velocity of mass center of i-th segment relative to the proximal endpoint

$\boldsymbol{a}_{Gi-p}$: acceleration of mass center of i-th segment relative to the proximal endpoint

$\boldsymbol{v}_{d-p}$: velocity of the distal endpoint relative to the proximal endpoint

$\boldsymbol{v}_{p}$: velocity of the proximal endpoint

$\boldsymbol{f}_{p}$: external joint force acting at the proximal endpoint

$\boldsymbol{v}_d$: velocity of the distal endpoint

$\boldsymbol{f}_d$: force acting at the distal endpoint

$\boldsymbol{\omega}_i$: segmental angular velocity of i-th segment

$\boldsymbol{n}_{Gi}$: rate of change of angular momentum of i-th segment

$\boldsymbol{T}$: vector of muscular torque

T_k: muscular torque of k-th joint

$\dot{\theta}_k$: joint angular velocity of k-th joint

Acknowledgement

This work was supported by JSPS KAKENHI [grant number JP15K01584].

References

Aguinaldo, A. L. and Escamilla, R. F. (2020). Induced power analysis of sequential body motion and elbow valgus load during baseball pitching. *Sports Biomech.* 1-13.

Bernstein, N.A. (1967). *Co-ordination and regulation of movements.* Oxford, UK: *Pergamon Press.*

Bunn, J. (1972). *Scientific Principles of Coaching.* Englewood Cliffs, NJ: Prentice-Hall.

Dounskaia, N. (2005). The internal model and the leading joint hypothesis: Implications for control of multi-joint movements. *Exp. Brain Res.* 166, 1-16.

Dounskaia, N. (2011). Control of human limb movements: The leading joint hypothesis and its practical applications. *Exerc Sport Sci Rev.* 38, 201-208.

Dounskaia, N. and Shimansky, Y. (2006). Strategy of arm movement control is determined by minimization of neural effort for joint coordination. *Exp. Brain Res*. 234, 1335–1350.

Escamilla, R., Fleisig, G., Barrentine, S., Andrews, J., and Moorman, C. 3rd. (2002). Kinematic and kinetic comparisons between American and Korean professional baseball pitchers. *Sports Biomech*. 1, 213–228.

Fregly B.J. and Zajac F.E. (1996). A state-space analysis of mechanical energy generation, absorption, and transfer during pedaling. *J. Biomech.* 29, 81-90.

Fleisig, G. S., Barrentine, S. W., Zheng, N., Escamilla, R. F., and Andrews, J. R. (1999). Kinematic and kinetic comparison of baseball pitching among various levels of development. *J. Biomech.* 32, 1371–1375.

Hatsopoulos, N.G., Olmedo, L. and Takahashi, K. (2010). Proximal-to-distal sequencing behavior and motor cortex. In *Motor Control: Theories, Experiments, and Applications* (ed. F. Danion and M.L. Latash), pp.159-176. New York: Oxford University Press.

Hill A.V. (1938) The heat of shortening and the dynamic constants of muscle. *Proc. R. Soc. B* 126, 136–195.

Hirashima, M., Kudo, K. and Ohtsuki, T. (2003). Utilization and compensation of interaction torques during ball-throwing movements. *J. Neurophysiol.* 89, 1784–1796.

Hirashima, M., Kudo, K., Watarai, K. and Ohtsuki, T. (2007). Control of 3D limb dynamics in unconstrained overarm throws of different speeds performed by skilled baseball players. *J. Neurophysiol.* 97, 680-691.

Hirashima, M., Yamane, K., Nakamura, Y. and Ohtsuki, T. (2008). Kinetic chain of overarm throwing in terms of joint rotations revealed by induced acceleration analysis. *J. Biomech.* 41, 2874-2883.

Isableu, B., and Berret, B. (2016). Adaptive use of interaction torque during arm reaching movement from the optimal control viewpoint. *Sci. Rep*. *6*, 38845.

Kim, Y.K., Hinrichs, R. N. and Dounskaia, N. (2009). Multicomponent control strategy underlying production of maximal hand velocity during horizontal arm swing. *J. Neurophysiol.* 102, 2889-2899.

Kreighbaum, E. and Barthels, K. M. (1996). *Biomechanics: A qualitative approach for studying human movement. fourth edition* (pp. 335-345). Needham, MA: Allyn & Bacon.

Martin, C., Bideau, B., Bideau, N., Nicolas, G., Delamarche, P. and Kulpa, R. (2014). Energy flow analysis during the tennis serve: comparison between injured and noninjured tennis players. *Am. J. Sports Med*. 42, 2751-2760.

Naito, K. and Maruyama, T. (2008). Contributions of the muscular torques and motion-dependent torques to generate rapid elbow extension during overhand baseball pitching. *Sports Eng*. 11, 47-56.

Naito, K., Takagi, H. and Maruyama, T. (2011). Mechanical work, efficiency and energy redistribution mechanisms in baseball pitching. *Sports* Technol. 4, 48–64.

Naito, K., Takagi, T., Kubota, H. and Maruyama, T. (2017). Multi-body dynamic coupling mechanism for generating throwing arm velocity during baseball pitching. *Hum Mov Sci.* 54, 363-376.

Naito, K., Wakayama, A., Kubota, H. and Maruyama, T. (2018). Energy distribution mechanism and open-kinetic-chain characteristics of the upper body system in female volleyball spiking. *Proc. Inst. Mech. Eng. Pt. P J. Sports Eng. Tech. 232*, 79-93

Putnam, C. A. (1993). Sequential motions of body segments in striking and throwing skills: descriptions and explanations. *J. Biomech.* 26, 125-135.

Reid, M., Giblin, G. and Whiteside, D. (2015). A kinematic comparison of the overhand throw and tennis serve in tennis players: How similar are they really?. *J. Sports Sci. 33*, 713-723.

Roach, N. T. and Lieberman, D. E. (2014). Upper body contributions to power generation during rapid, overhand throwing in humans. *J. Exp. Biol*. *217*, 2139-2149.

Roach, N. T., Venkadesan, M., Rainbow, M. J. and Lieberman, D. E. (2013). Elastic energy storage in the shoulder and the evolution of high-speed throwing in Homo. Nature 498, 483-486.

Serrien, B. and Baeyens, J.P. (2017). The proximal-to-distal sequence in upper-limb motions on multiple levels and time scales. *Hum Mov Sci.* 55, 156-171.

Sparrow, W.A., Hughes, K.M., Russell, A.P. and Le Rossignol, P.F. (1999). Effects of practice and preferred rate on perceived exertion, metabolic variables and movement control. *Hum Mov Sci.* 18, 137-153.

Van den Tillaar, R., and Ettema, G. (2009). Is there a proximal-to-distal sequence in overarm throwing in team handball?. *J. Sports Sci.* 27, 949-955.

Wagner, H., Pfusterschmied, J., Von Duvillard, S. P. and Müller, E. (2012). Skill-dependent proximal-to-distal sequence in team-handball throwing. *J. Sports Sci*. *30*, 21-29.

Winter D.A. (2009). *Biomechanics and motor control of human movement. fourth edition* (pp. 14-44). Hoboken, NJ: John Wiley & Sons.

Zajac, F.E., Neptune, R.R. and Kautz, S. A. (2002). Biomechanics and muscle coordination of human walking. Part I: Introduction to concepts, power transfer, dynamics and simulations. *Gait Posture*. 16, 215-232.

Zatsiorsky, V.M. (2002). *Kinetics of human motion* (pp. 542-547). Champaign, IL: Human kinetics.

Figures and Tables:

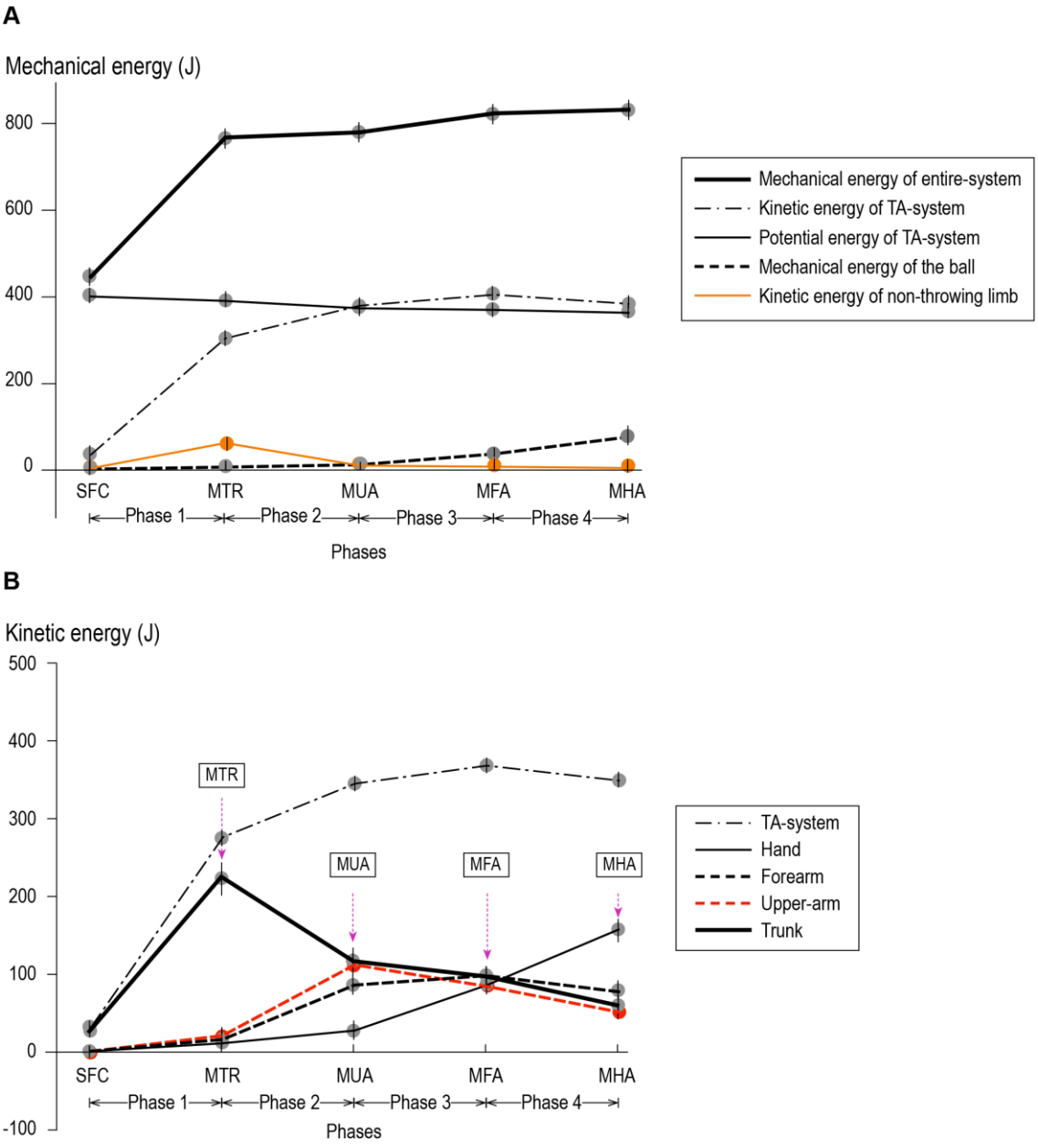

Fig. 1. Mean of mechanical energy-time profile for the system and limbs (N=80).

(A) Mechanical energy of the entire-system, trunk–throwing arm system, non-throwing limb, and ball. (B) Kinetic energy of the trunk and throwing-side upper-arm, forearm, and hand. SFC, MTR, MUA, MFA, and MHA indicate the instants of the stride foot contact and maximum kinetic energy of the trunk, upper-arm, forearm, and hand. Phases 1-4 are defined by the periods between SFC and MTR, MTR and MUA, MUA and MFA, and MFA and MHA.

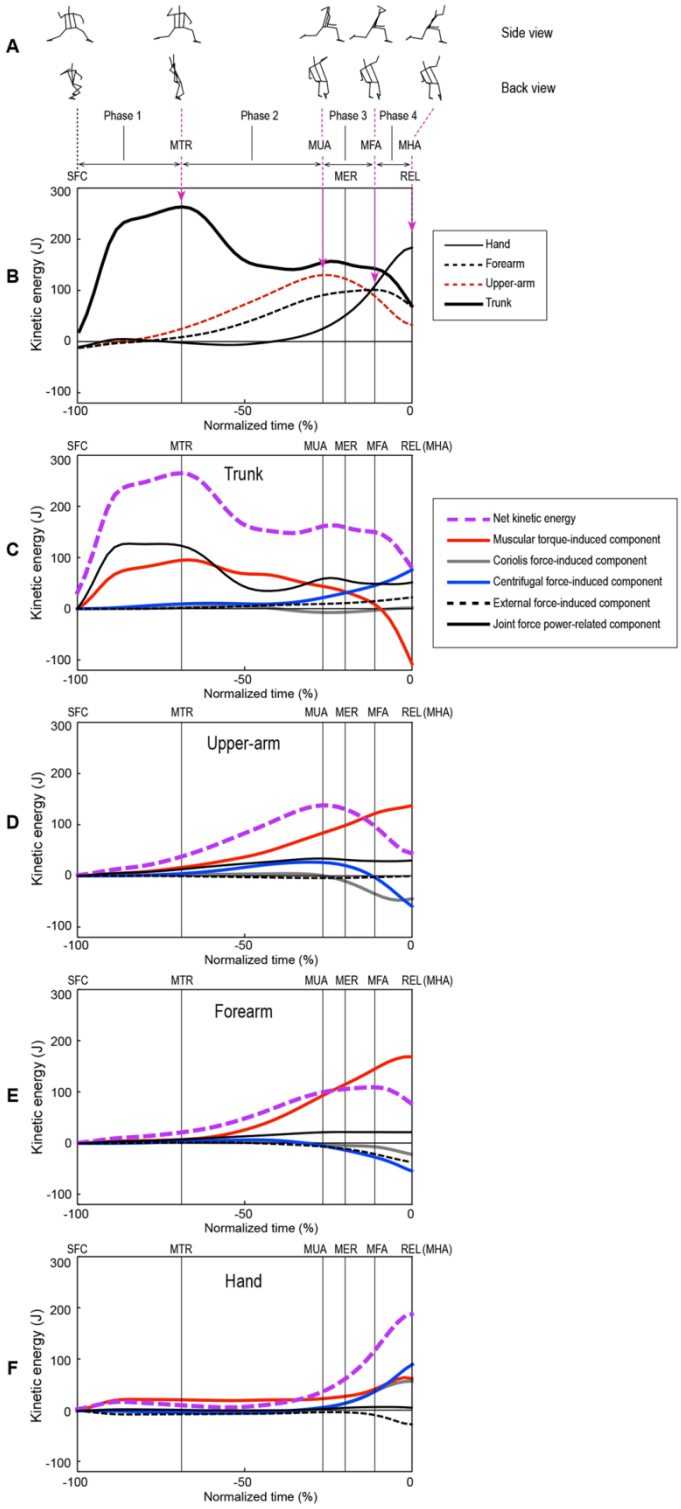

Fig. 2. Representative examples of the segment kinetic energy and decomposition of that energy into the causal factor-induced components of a single participant. (A) Stick figure illustration of the throwing movement. (B) Kinetic energy of the trunk and throwing upper-arm, forearm, and hand. C-F indicate the trunk, upper-arm, forearm, and hand kinetic energy and causal factor-induced components of those energies. The definitions of four phases and all abbreviations are the same as those in Fig. 1. MER is the instant of shoulder maximum external rotation. The gyroscopic moment-, gravity-, and trunk linear acceleration-induced components are not presented because of the small contributions of those components.

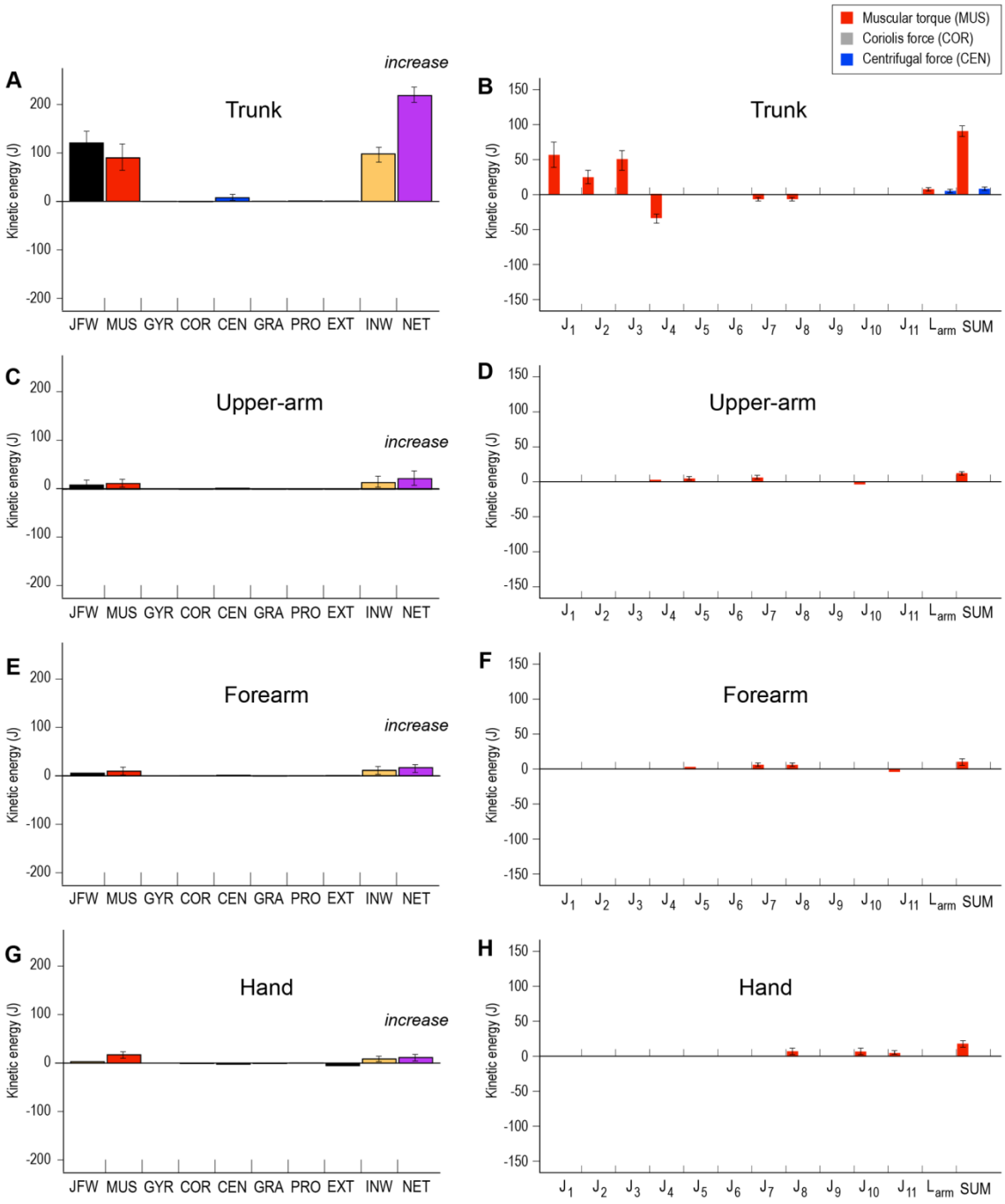

Control indices (energy-generation: 100.0±0.0 %, energy-transfer: 0.0±0.0 %)

Fig. 3. Change in the segment kinetic energy during "phase 1" and its decomposition of that energy into the causal factor-induced components (N=80).

A, C, E, and G show the mean of the net and each factor-induced kinetic energy of the trunk, upper-arm, forearm, and hand. B, D, F, and H show the mean of the individual joint contributions of the muscular torque-, Coriolis force-, and centrifugal force-induced components to the change in kinetic energy of the trunk, upper-arm, forearm, and hand. NET represents the net kinetic energy of the segments. MUS, GYR, COR, CEN, GRA, PRO, and EXT indicate the muscular torque-, gyroscopic moment-, Coriolis force-, centrifugal force-, gravity-, trunk linear acceleration-, external force (applying to the ball)-induced kinetic energy. INW represents internal work corresponding to the sum of those factor-induced components. JFW represents the contribution of the external joint force power-related component. J_1 - J_4 indicate the trunk backward/forward tilt, right/left tilt, and forward/ backward rotation, and scapula right/left tilt. J_5 - J_{11} indicate the shoulder external/internal rotation, adduction/abduction, and horizontal adduction/abduction, elbow extension/flexion, forearm supination/pronation, and wrist extension/flexion and ulnar/radial deviation of the throwing-side arm. L_{arm} indicates the sum of the non-throwing (left) arm joint contributions. SUM indicate the sum of all joint components. Energy-generation and energy-transfer of control indices are 100.0±0.0% and 0.0±0.0%, respectively.

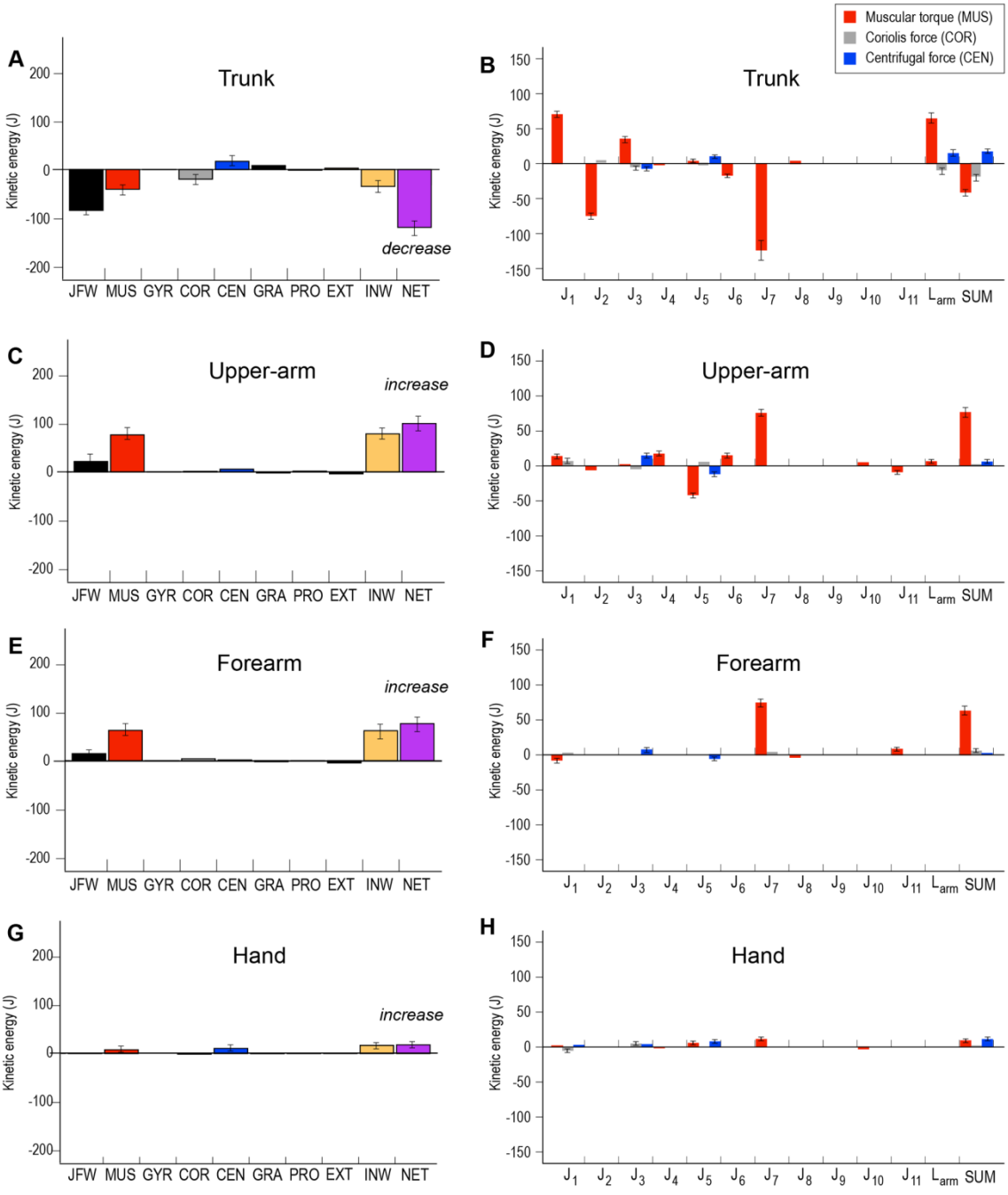

Fig. 4. Change in the segment kinetic energy during "phase 2" and its decomposition of that energy into the causal factor-induced components (N=80). A, C, E, and G show the mean of the net and each factor-induced kinetic energy of the trunk, upper-arm, forearm, and hand. B, D, F, and H show the mean of the individual joint contributions of the muscular

torque-, Coriolis force-, and centrifugal force-induced components to the change in kinetic energy of the trunk, upper-arm, forearm, and hand. The definitions of joint numbers and abbreviations are the same as those in Fig. 3. Energy-generation and energy-transfer of control indices are 38.7±12.0% and 61.3±15.0%, respectively.

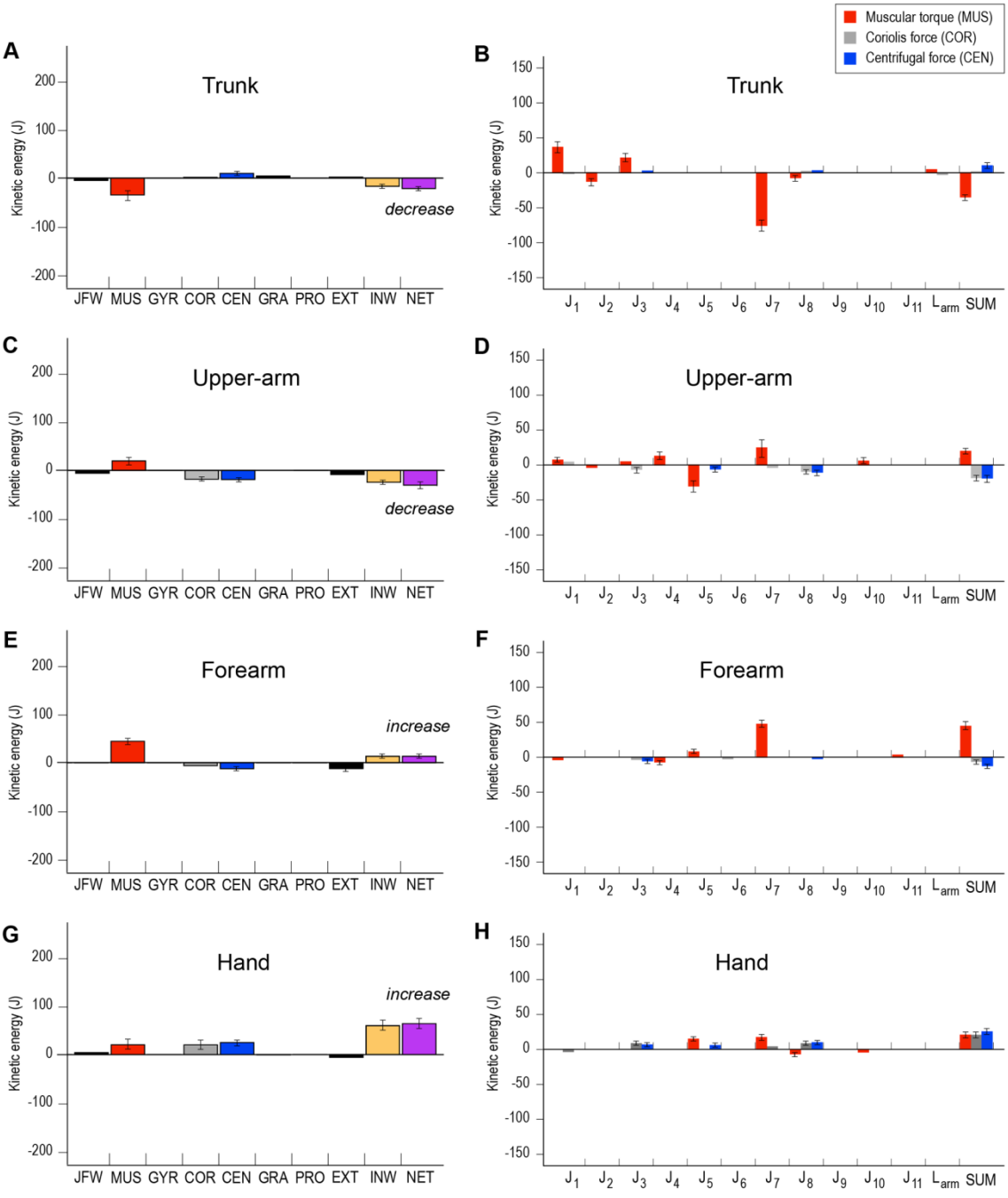

Fig. 5. Change in the segment kinetic energy during "phase 3" and its decomposition of that energy into the causal factor-induced components (N=80). A, C, E, and G show the mean of the net and each factor-induced kinetic energy of the trunk, upper-arm, forearm, and hand. B, D, F, and H show the mean of the individual joint contributions of the muscular

torque-, Coriolis force-, and centrifugal force-induced components to the change in kinetic energy of the trunk, upper-arm, forearm, and hand. The definitions of joint numbers and abbreviations are the same as those in Fig. 3. Energy-generation and energy-transfer of control indices are 32.8±12.5% and 67.2±11.0%, respectively.

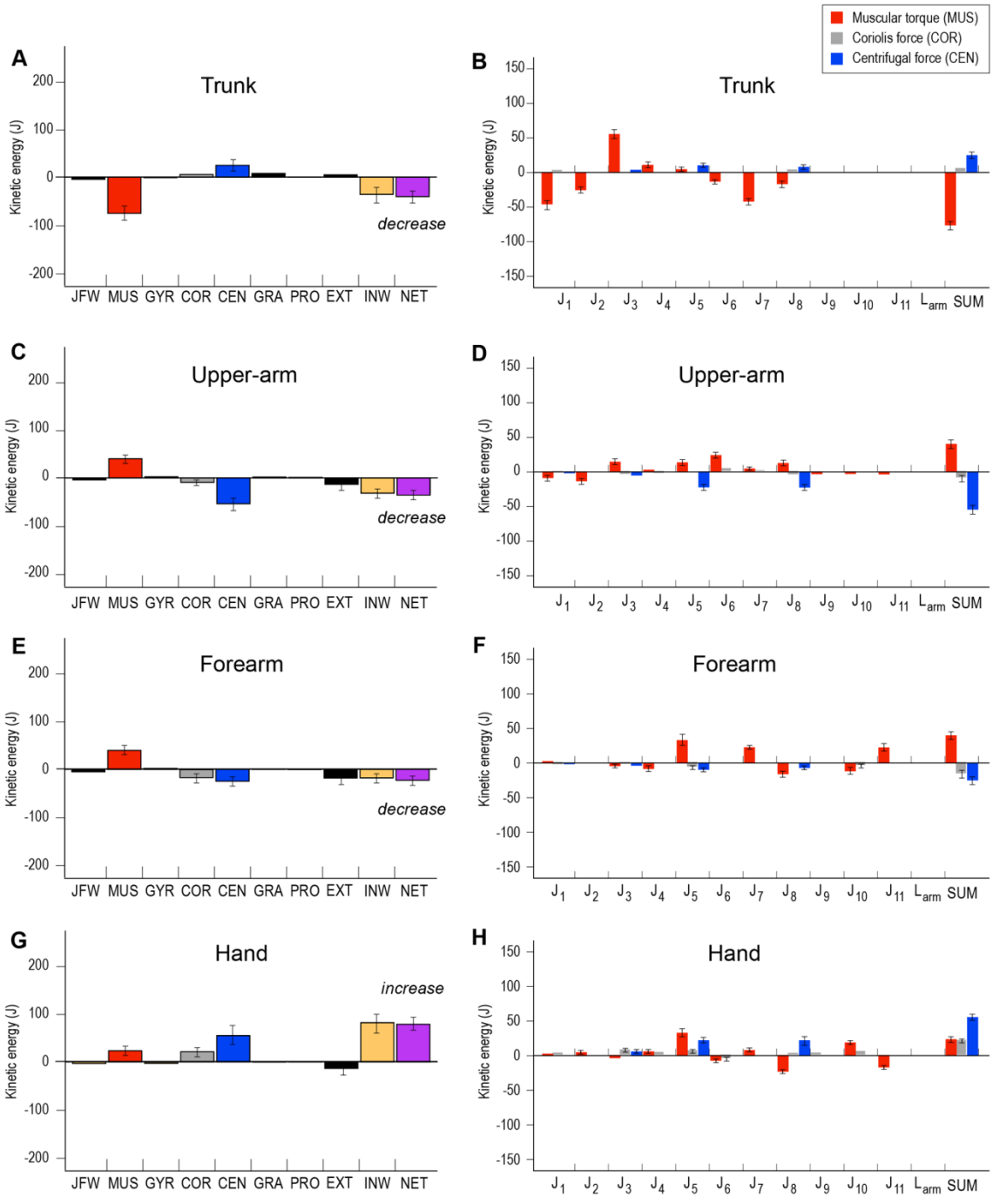

Fig. 6. Change in the segment kinetic energy during "phase 4" and its decomposition of that energy into the causal factor-induced components (N=80). A, C, E, and G show the mean of the net and each factor-induced kinetic energy of the trunk, upper-arm, forearm, and

hand. B, D, F, and H show the mean of the individual joint contributions of the muscular torque-, Coriolis force-, and centrifugal force-induced components to the change in kinetic energy of the trunk, upper-arm, forearm, and hand. The definitions of joint numbers and abbreviations are the same as those in Fig. 3. Energy-generation and energy-transfer of control indices are 0.0±0.5% and 100.0±0.5%, respectively.

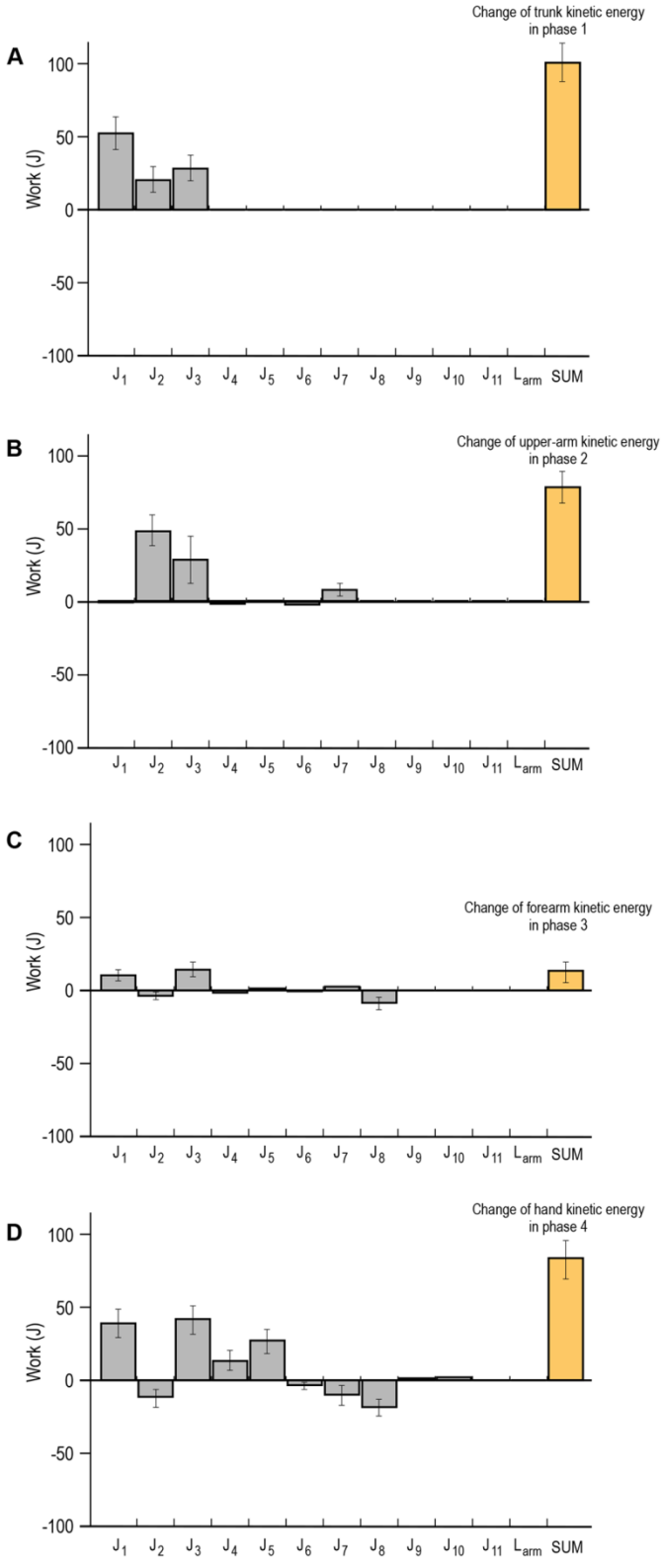

Fig. 7. Muscle work resulting in the change in kinetic energy of different segments during specific phases (N=80). A-D show muscle internal work expended on the increase of 'the trunk kinetic energy of phase 1', that of 'upper-arm kinetic energy of phase 2', that of 'forearm kinetic energy of phase 3', and that of 'hand kinetic energy of phase 4'. The definitions of joint numbers, L_{arm}, and SUM are the same as those in Fig. 3.

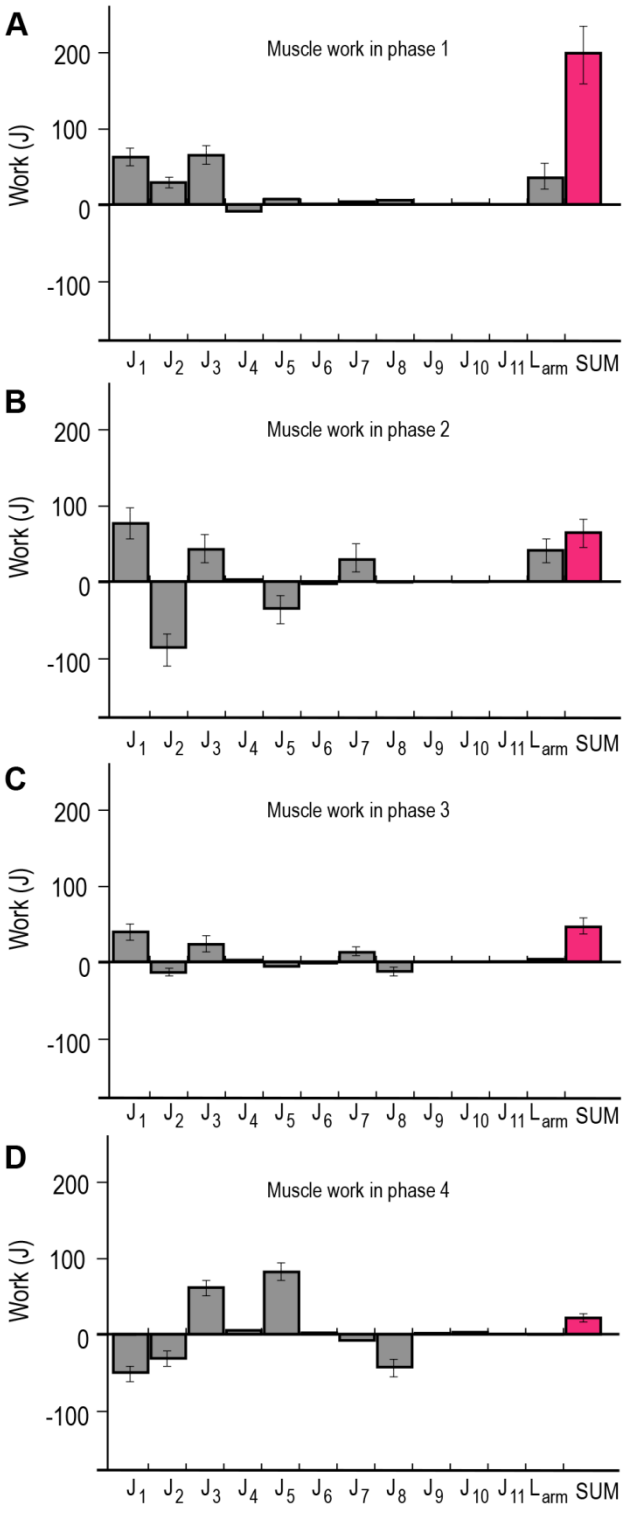

Fig. 8. Muscle work generated in each different phase (N=80). A-D show the muscle work generated in phases 1-4. The definitions of joint numbers, L_{arm}, and SUM are the same as those in Fig. 3.

Table 1. Mean value and normalized time of kinematic and energetic variables (N=80).

	Mean	SD
Maximum angular velocity (degree/s)		
Trunk forward rotation	1253	125
Normalized time (%)	*51*	*5*
Shoulder internal rotation	6030	592
Normalized time (%)	*101*	*1*
Shoulder horizontal adduction	711	142
Normalized time (%)	*62*	*28*
Elbow extension	2192	218
Normalized time (%)	*94*	*2*
Maximum kinetic energy (J)		
Trunk	249	35
Normalized time (%)	*19*	*4*
Upper-arm	109	10
Normalized time (%)	*64*	*3*
Forearm	83	8

Normalized time (%)		*83*	*3*
Hand	180	32	
Normalized time (%)		*100*	*0*

Table 2. Muscle work done by individual joint and work expenditure on the mechanical energy applied to the system and ball through overall throwing phase (N=80).

Joint	J_1	J_2	J_3	J_4	J_5	J_6	J_7	J_8	J_9	J_{10}	J_{11}	L_{arm}	Sum
Kinetic energy													
Segment													
Trunk	42.8	-87.0	54.1	0.0	0.0	0.0	0.0	0.0	0.0	0.0	0.0	0.0	9.9
	(10.7)	(6.0)	(7.6)	(0.0)	(0.0)	(0.0)	(0.0)	(0.0)	(0.0)	(0.0)	(0.0)	(0.0)	(5.2)
Upper-arm	-61.6	46.2	27.2	24.5	34.3	0.4	14.0	0.0	0.0	0.0	0.0	0.0	36.0
	(7.4)	(7.1)	(3.4)	(1.5)	(1.4)	(1.0)	(2.9)	(0.0)	(0.0)	(0.0)	(0.0)	(0.0)	(4.0)
Forearm	11.5	14.5	57.1	- 3.0	- 2.1	4.2	16.9	- 30.1	0.0	0.0	0.0	0.0	68.9
	(15.6)	(10.1)	(7.4)	(3.4)	(2.6)	(1.7)	(2.8)	(2.9)	(0.0)	(0.0)	(0.0)	(0.0)	(4.7)
Hand	92.6	-29.3	84.0	25.2	9.8	-4.7	5.4	-19.7	1.6	2.2	0.1	0.0	167.2
	(16.1)	(7.2)	(15.7)	(3.4)	(3.1)	(1.4)	(2.9)	(2.5)	(0.2)	(0.6)	(0.2)	(0.0)	(36.7)
Non-throwing limb	31.2	-27.1	-65.4	-10.9	0.0	0.0	0.0	0.0	0.0	0.0	0.0	75.3	3.2
	(9.0)	(1.3)	(14.6)	(2.8)	(0.0)	(0.0)	(0.0)	(0.0)	(0.0)	(0.0)	(0.0)	(10.2)	(4.8)

System potential energy

-24.9	-5.7	0.0	3.2	0.1	0.6	0.4	0.3	0.0	0.1	0.0	-2.2	-28.1
(2.8)	(3.5)	(0.0)	(0.0)	(0.0)	(0.0)	(0.0)	(0.0)	(0.0)	(0.0)	(0.0)	(0.0)	(5.3)

Mechanical energy of ball

35.4	-14.9	33.3	10.7	5.1	-2.8	0.0	-1.5	0.0	0.7	0.6	5.5	72.1
(16.0)	(3.9)	(5.4)	(2.4)	(1.5)	(0.8)	(0.0)	(0.7)	(0.0)	(0.2)	(0.2)	(3.0)	(12.4)

Total muscle work

126.9	-103.3	190.4	0.7	47.2	-2.3	36.6	-51.1	1.6	2.9	0.7	78.6	329.2
(57.5)	(25.9)	(47.5)	(5.5)	(6.8)	(3.3)	(16.9)	(24.6)	(0.2)	(1.6)	(0.2)	(38.8)	(43.6)